Luminescent 1,8-Naphthalimide-Derived Re^I Complexes: Syntheses, Spectroscopy, X-ray Structure and Preliminary Bioimaging in Fission Yeast Cells

Emily E. Langdon-Jones,[a] Catrin F. Williams, [b,c] Anthony J. Hayes,[c] David Lloyd,[c] Simon J. Coles,[d] Peter N. Horton,[d] Lara M. Groves,[a] and Simon J. A. Pope*[a]

Abstract: A series of picolyl-functionalised, fluorescent 1,8-naphthalimide ligands (L) have been synthesised and coordinated to Re^I to form luminescent cationic complexes of the general form *fac*-[Re(phen)(CO)$_3$(L)]BF$_4$. The complexes were characterised by using a range of spectroscopic and analytical techniques. One example of a complex was also characterised in the solid-state by using single-crystal X-ray diffraction, revealing a distorted octahedral coordination sphere at Re^I and Re–C/Re–N bond lengths within the expected ranges. All ligands were shown to be fluorescent, with the 4-amino derivatives showing intramolecular charge transfer in the visible region (511–534 nm). The complexes generally showed a mixture of ligand-centred and/or ^{3}MLCT emission depending upon the nature of the coordinated 1,8-naphthalimide ligand. For selected complexes, confocal fluorescence microscopy was undertaken by using fission yeast cells (*Schizosaccharomyces pombe*) and showed that the structure of the 1,8-naphthalimide ligand influences the uptake and localisation of the rhenium complex.

Introduction

The 1,8-naphthalimide structural motif is a remarkably functional moiety that has found utility in a wide variety of applications. Such derivatives can be synthesised in a stepwise manner allowing control over functionalisation. The electronic proper-ties of substituted 1,8-naphthalimides have been utilised in a wide range of molecular architectures, from multichromophoric light harvesting arrays[1] to the design of fluorescent sensors[2] (for a multiplicity of analytes including, metal cations, anions, pH and biomolecules). 1,8-Naphthalimide based fluorophores are known to possess tuneable emission in the visible region (depending upon the nature and position of substituent), to-gether with high photostability. For donor functionalised 1,8-naphthalimides, the nature of the emitting state is usually an intramolecular charge transfer (ICT), which results in solvato-chromic behaviour. The fluorescence behaviour of such systems has been successfully applied to the design of probes for fluo-rescence cell imaging,[3] wherein high quantum yields and large Stokes' shifts are advantageous. Beyond their electronic proper-

ties, other very important uses for 1,8-naphthalimides include as DNA binding probes,[4] and as components of therapeutics (for example, amonafide[5]), including those with anticancer[6] properties. 1,8-Naphthalimides have also found far-ranging application in coordination chemistry,[7] including, for example, in the development of tyrosine kinase inhibitors,[8] lanthanide-based 3D supramolecular frameworks,[9] luminescent lanthanide assemblies,[10] and DNA-interacting organometallics.[11] In recent years we have studied the combination of 1,8-naphthalimide derived fluorophores with coordination complexes (e.g. with Au^I) and investigated the resultant species in the context of cell imaging studies.[12] Following on from this work we present our findings on the development of mixed-ligand Re^I complexes that incorporate a picolyl-functionalised 1,8-naphthalimide ligand. In recent years, organometallic Re^I com-plexes have shown great utility in bioimaging studies using confocal fluorescence microscopy,[13] including examples which demonstrate ligand-derived control over intracellular localisation. Herein, the synthesis and spectroscopic characterisation of a series of 1,8-naphthalimide functionalised ligands are de-scribed, together with their complexation to Re^I to form complexes of the type *fac*-[Re(phen)(CO)$_3$(L)]BF$_4$ (where phen = 1,10-phenanthroline). Some preliminary cell imaging studies are also presented showing the applicability of such systems to bioimaging using fluorescence microscopy.

Results and Discussion

Ligand Synthesis and Characterisation

Ligands (**L1–7**) were isolated, through one or two steps (Scheme 1), from commercially available 4-chloro-1,8-

[a] *School of Chemistry, Cardiff University, Cardiff, CF10 3AT, UK*
E-mail: PopeSJ@Cardiff.ac.uk
www.cardiff.ac.uk/chemistry

[b] *School of Engineering, Cardiff University, Cardiff, CF24 3AA, UK*
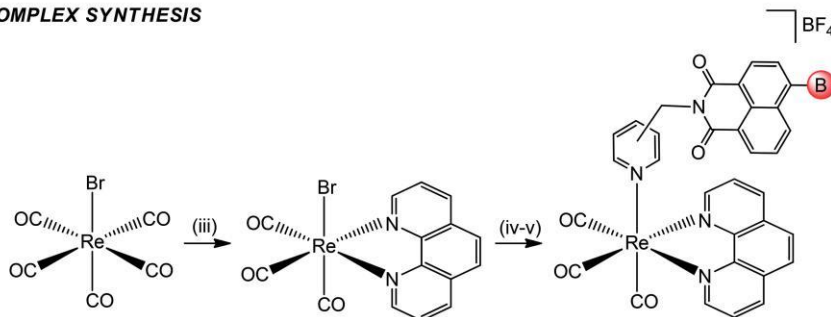
[c] *School of Biosciences; Cardiff University, Cardiff, CF10 3AT, UK*

[d] *UK National Crystallographic Service, Chemistry, Faculty of Natural and Environmental Sciences, University of Southampton, Highfield, Southampton, SO17 1BJ, England, UK*

A 3-picolyl, 4-picolyl

B H, Cl, piperidine, benzylamine

L1 L2 L3 L4 L5 L6 L7

COMPLEX SYNTHESIS

BF₄
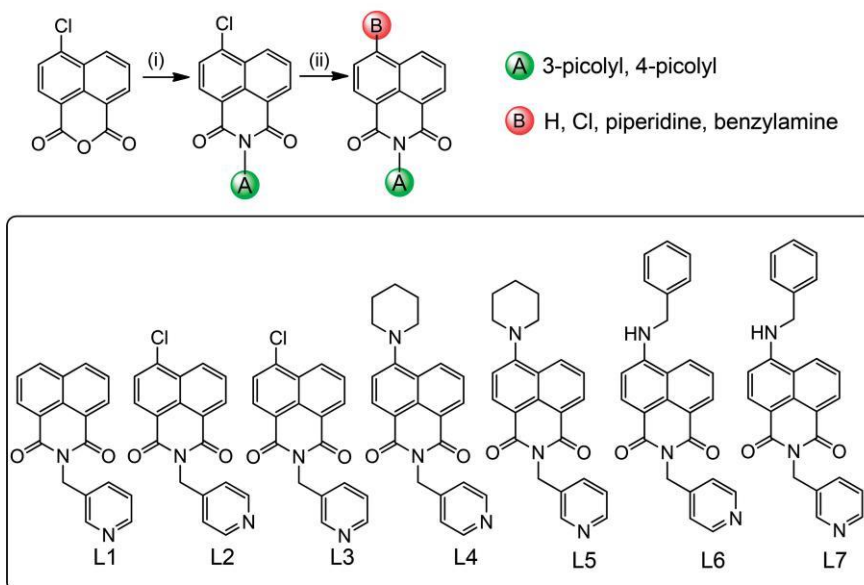
Scheme 1. Synthetic route to the ligands (shown inset) and complexes: (i) 3-picolylamine or 4-picolylamine, EtOH, heat; (ii) piperidine or benzylamine, DMSO, heat; (iii) 1,10-phenanthroline, toluene, heat; (iv) AgBF₄, MeCN; (v) L1–L7, CHCl₃, heat.

naphthalic anhydride. **L1**[14] has been previously reported. The first step involved conversion to 4- or 3-picolyl 4-chloro-substituted species (**L1–3**). **L2–3** could be further functionalised by substitution at the 4-position with either piperidine or benzylamine. Reaction was achieved by heating in DMSO at 70 **°C** with four equivalents of the respective amine. The successful formation of **L4–7** was easily determined by ^{1}H and ^{13}C{^{1}H} NMR spectroscopy. For **L6** and **L7** there was a characteristic NH resonance (broad triplet) at *ca.* 5.7 ppm. All ligands were characterised by high resolution mass spectrometry (HRMS) (ES$^+$), showing the [M + H]$^+$ cation peak in all cases. IR spectroscopy showed two C=O bands at ca. 1690 and 1650 cm^{-1}, with **L2–3** having an additional strong peak at *ca.* 780 cm^{-1} (C–Cl) and **L6–7**, with a secondary amine, showing the expected peaks for the N–H stretch and bend modes ca. 3300 and 1560 cm^{-1}.

Complex Synthesis and Characterisation

The complexes were synthesised (Scheme 1) by heating *fac*-[Re(phen)(CO)₃(MeCN)]BF₄ with the appropriate ligand in chloroform under a dinitrogen atmosphere for 12 hours.[15] The Re^I complexes were fully characterised by ^{1}H and ^{13}C{^{1}H} NMR, IR, UV/Vis. spectroscopy and HRMS. ^{1}H NMR spectroscopy re-

vealed a minor shift (*ca.* 0.2 ppm) of the N$_{imide}$–CH_2 resonance upon coordination to Re^I. ^{13}C{^{1}H} NMR spectroscopy distinguished the metal bound carbonyls (*ca.* 185–195 ppm) and ligand based C=O resonances (*ca.* 160 ppm). HRMS (ES$^+$) showed a cluster of peaks for the [M]$^+$ ion and also commonly [M + MeCN]$^+$. The presence of Re^I was confirmed by the expected isotopic distribution (^{185}Re, 37.4 %; ^{187}Re 62.6 %). Furthermore, IR spectroscopy confirmed the proposed geometry with metal carbonyl stretches *ca.* 2030–1900 cm^{-1} and a slight shift in the imide carbonyl peaks at lower wavenumber values. IR spectro-scopy data supported the assignment of an approximated C_{3v} or C_s symmetry at the complex, which predict either two or three carbonyl stretches for *fac*-[Re(CO)₃(N^N)(X)] complexes. All complexes possessed an additional peak at ca. 1050 cm^{-1} as-signed to the BF₄$^-$ counter anion.

X-ray Crystal Structure of *fac*-[Re(phen)(CO)₃(L4)]BF₄

A single-crystal X-ray structure determination was obtained for *fac*-[Re(phen)(CO)₃(**L4**)]BF₄ (Figure 1). Orange plate crystals were obtained via vapour diffusion of diethyl ether into a concentrated MeCN solution of the complex. The data collection parameters and refinement details are shown in Table 1; bond

lengths and bond angles are shown in ESI, Table S1. There are four unique complex cation moieties in the asymmetric unit. Data analysis confirmed the proposed structure with a slightly distorted octahedral coordination geometry for Re^I, involving a *fac*-tricarbonyl arrangement, a chelating phenanthroline ligand and an axially N-coordinated picolyl-naphthalimide moiety (**L4**). The bond lengths associated with the coordination sphere are typical of related Re^I complexes.[16] The Re–CO distances lie within the range 1.86–1.95(2) Å, whilst the Re–N distances were typically longer at 2.173–2.217(14) Å. It is noteworthy that the Re–N bond lengths to the axial monodentate pyridine are very similar to those associated with the chelating phenanthroline. This could be explained by the lack of distortion along the axial plane [C_{ax}–Re–N_{ax} 177.4–179.2(6)°] compared to the equatorial

plane [C_{eq}–Re–N_{eq} 170.1–173.0(7)° and 175.1–175.6(6)°], result-ing in a marginal strengthening of the Re–N_{py} bond and desta-bilisation of the Re–N_{phen} bond. Interestingly this example shows that the naphthalimide unit of **L4** is positioned over, and relatively co-planar to, the chelating phenanthroline ligand. However, this arrangement does not appear to be an intra-molecular π–π stacking interaction (C_{naph}–C_{phen} 7.26–8.40 Å) and likely results from crystal packing effects.

Table 1. Data collection parameters for the X-ray structure of *fac*-[Re(phen)(CO)$_3$(**L4**)]BF$_4$.

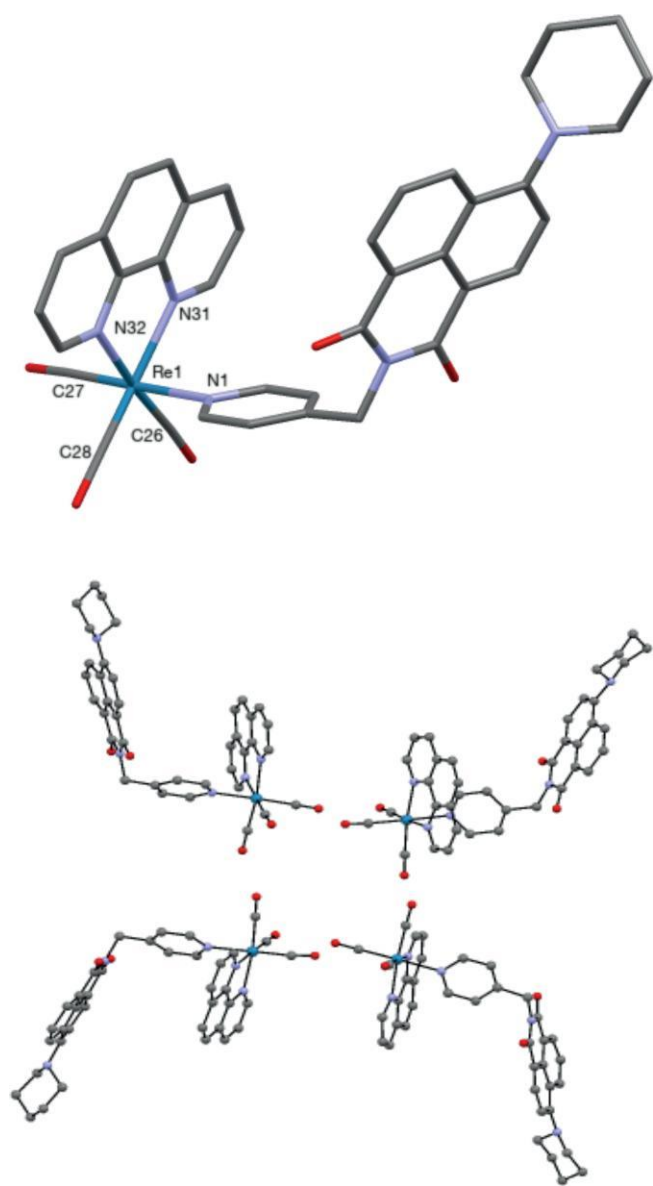| Formula	$C_{38}H_{29}BF_4N_5O_5Re$
$D_{calcd.}$ /g cm^{-3}	1.468
μ /mm^{-1}	3.020
Formula weight	908.67
Colour	Orange
Shape	plate
Size /mm	0.09 × 0.08 × 0.03
T /K	100(2)
Crystal system	orthorhombic
Flack parameter	0.220(9)
Hooft parameter	0.221(4)
Space group	*Fdd*2
a /Å	22.9167(16)
b /Å	51.006(4)
c /Å	56.261(4)
α /°	90
/°	90
γ /°	90
V /Å^3	65763(8)
Z	64
Z'	4
Wavelength /Å	0.71075
Radiation type	Mo-K_α
Θ_{min} /°	2.345
Θ_{max} /°	27.481
Measured refl.	134986
Independent refl.	37115
Reflections used	25303
R_{int}	0.0799
Parameters	2128
Restraints	3130
Largest peak	2.531
Deepest hole	−1.304
GooF	1.006
wR_2 (all data)	0.1446
wR_2	0.1269
R_1 (all data)	0.0941
R_1	0.0555

Figure 1. X-ray crystal structure of one moiety of *fac*-[Re(phen)(CO)$_3$(**L4**)]BF$_4$ (top) with ellipsoids at 50 % occupancy, and (bottom) the four different moie-ties of the asymmetric unit of the complex. Solvent, counter anions and hydrogen atoms are omitted.

Electronic Properties of the Ligands and Complexes

Table 2 shows the UV/Vis. absorption properties of the free li-gands and complexes. All ligands possessed strong π–π* bands below 350 nm (Figure 2). For **L1–3**, the lowest energy peak is vibronically structured and associated with the naphthalimide core. The addition of the 4-amino substituent induced an addi-tional unstructured band around 410–490 nm which is assigned to an intramolecular charge transfer (ICT), formally of n-π* char-acter. The ICT band can be weakened by a lack of planarity between the naphthalimide ring and the 4-amino sub-stituent.[17] The wavelength of the ICT absorption was batho-chromically shifted for the benzylamine derivatives.

Table 2. Absorption and luminescence properties of the ligands and com-plexes.

Compound[a]	λ_{abs} /nm[b]	λ_{em} /nm[a,c]	τ /ns[d]
L1	344	381	< 1
L2	340	392	9
L3	340	392	1
L4	411	534	< 1
L5	410	534	< 1
L6	429	512	10
L7	428	511	10
[Re(CO)₃(phen)(**L1**)]BF₄	345	528	190
[Re(CO)₃(phen)(**L2**)]BF₄	340	515	4, 40 (60 %)
[Re(CO)₃(phen)(**L3**)]BF₄	340	515	8, 73 (75 %)
[Re(CO)₃(phen)(**L4**)]BF₄	408	537	< 1, 7 (51 %)
[Re(CO)₃(phen)(**L5**)]BF₄	406	534	< 1, 16 (66 %)
[Re(CO)₃(phen)(**L6**)]BF₄	431	514	5, 10 (47 %)
[Re(CO)₃(phen)(**L7**)]BF₄	431	511	< 1, 10 (79 %)

[a] MeCN. [b] Lowest energy absorption. [c] λ_{exc} = 425 nm, 5 × 10^{-5} M. [d] λ_{exc} = 295 or 459 nm.

Figure 3. A comparison of the UV/Vis. absorption spectra of **L5** and *fac*-[Re(phen)(CO)₃(**L5**)]BF₄.
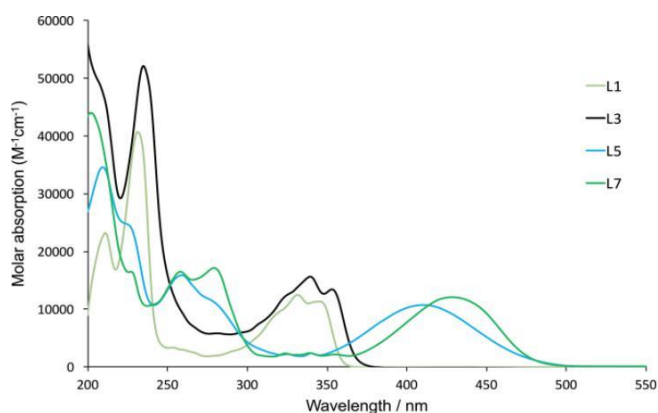

Figure 2. A comparison of the UV/Vis. absorption spectra for **L1**, **L3**, **L5** and **L7**.

For all Re^I complexes the absorption spectra were highly ligand dominated with the intense (ca. 10000 M^{-1} cm^{-1}) ICT transition overlapping with the anticipated ^{1}M$_{Re}$L$_{phen}$CT peak expected[18] of Re^I–phen complexes at 340–400 nm. Furthermore, the π–π* absorptions < 350 nm possessed higher molar absorp-tion coefficients compared to the free ligands due to the sum-mative effects of the phenanthroline and naphthalimide chromophores (Figure 3). The λ_{max} values for the latter show very little variation from the free ligands, presumably due to the lack of conjugation between the naphthalimide unit and the metal binding site.

Solutions of all ligands were found to be luminescent (Table 2). Measurements on aerated MeCN solutions of **L1–3** resulted in a faintly vibronically structured band between 380–410 nm (λ_{exc} = 345 nm), assigned to a ^{1}π–π* emitting state. For the amine-substituted naphthalimides, **L4–7**, each possessed a broad, unstructured emission band at 510–530 nm (Figure 4 and Table 2). This band is more typical of a donor substituted naphthalimide species and consistent with an ICT character. The position of the ICT emission was dependent upon the nature of the 4-amino substituent (Figure 4), with the piperidine vari-ants (**L4**, **L5**) giving the longest wavelength shift. The ICT nature of the emission band was exemplified by measuring in a range
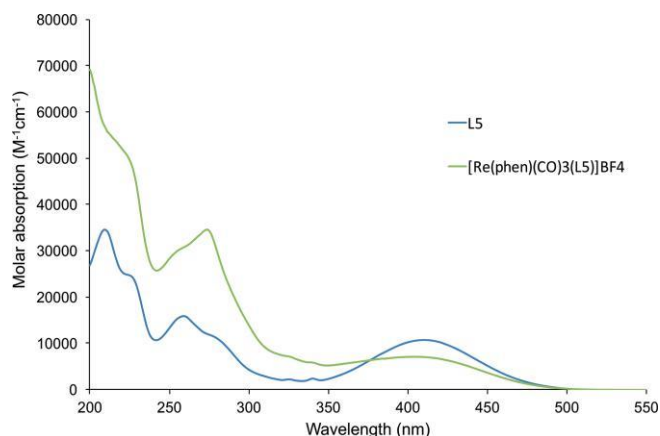
of solvents of different polarities whereupon the fluorophores demonstrated classical positive solvatochromism, as noted in our previous work.[12] A comparison of the excitation spectra for the different types of ligands showed clear differences. For example, comparing **L2** and **L7** revealed very different excita-tion profiles with the latter showing a broad peak ca. 440 nm, which was assigned to the ICT transition and thus correlates relatively well with the observed ICT absorption band (cf. λ_{abs} = 428 nm). Emission lifetime data on **L1**–**7** (Table 2) showed that the ligands were fluorescent in all cases (confirming a singlet emitting excited state) with lifetimes ≤ 10 ns; it was noted that the benzylamine derivatives had the longest lifetimes in the series.

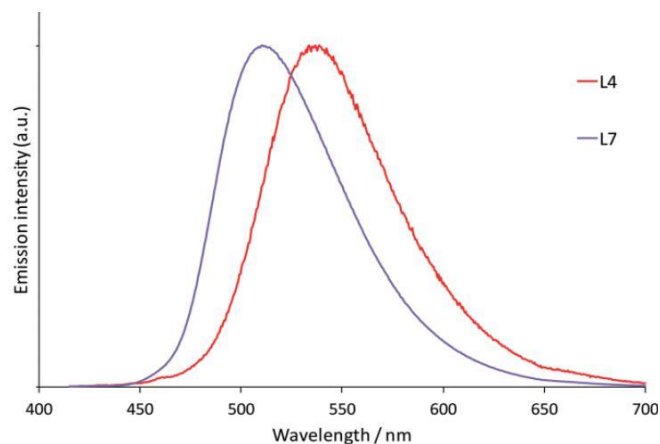Figure 4. A comparison of the emission spectra (λ_{exc} = 405 nm) of **L4** (red) and **L7** (purple).

For the complexes *fac*-[Re(phen)(CO)₃(**L1–3**)]BF₄ excitation at 405 nm gave a broad featureless peak ca. 515–528 nm. This excitation wavelength correlates with direct population of the ^{1}M$_{Re}$L$_{phen}$CT band since these complexes lack the naphthal-imide-localised ICT character. Using higher energy excitation bands resulted in dual emission for all three complexes. For example, Figure 5 shows the excitation wavelength dependent emission spectra for *fac*-[Re(phen)(CO)₃(**L1**)]BF₄. With compari-son to **L1**, the vibronically structured emission peak at 340–

440 nm can be attributed to naphthalimide-centred fluorescence, whilst the broad peak at 529 nm was assigned to the $^3M_{Re}L_{phen}CT$ transition. The corresponding lifetimes (aerated solvent) of these peaks confirm this assignment: with λ_{em} = 529 nm, the observed lifetime was 190 ns, which is consistent with cationic fac-[Re(phen)(CO)$_3$(L)]$^+$ type complexes,[19] while at λ_{em} = 385 nm the lifetime was <10 ns.[12] For fac-[Re(phen)(CO)$_3$(L2)]BF$_4$ and fac-[Re(phen)(CO)$_3$(L3)]BF$_4$ this $^3M_{Re}L_{phen}CT$ lifetime was shortened to 40 ns and 73 ns respectively, suggesting a partial quenching of the excited state possibly due to the nature of the axial ligand.[15]
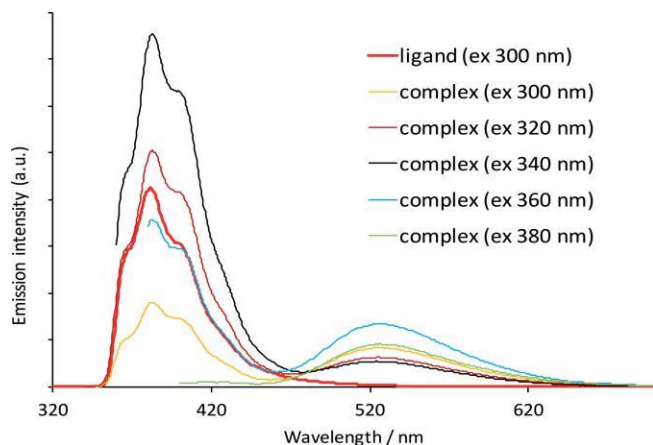

Figure 5. Emission spectra showing excitation wavelength dependence of fac-[Re(phen)(CO)$_3$(L1)]BF$_4$, together with a comparison to L1 (red trace).

For the other complexes in the series there was a close correlation with the emission wavelengths of the corresponding free ligands. Lifetime measurements gave luminescence decay profiles that fitted best to a dual component biexponential, and the major contributions from these decays were <20 ns. This suggests that any $^3M_{Re}L_{phen}CT$ character is strongly quenched, due to the presence of the substituted naphthalimide ligands. This might be explained by the partial overlap of the ICT naphthalimide absorption band with the expected $^3M_{Re}L_{phen}CT$ emission profile. In the cases of the benzylamine variants fac-
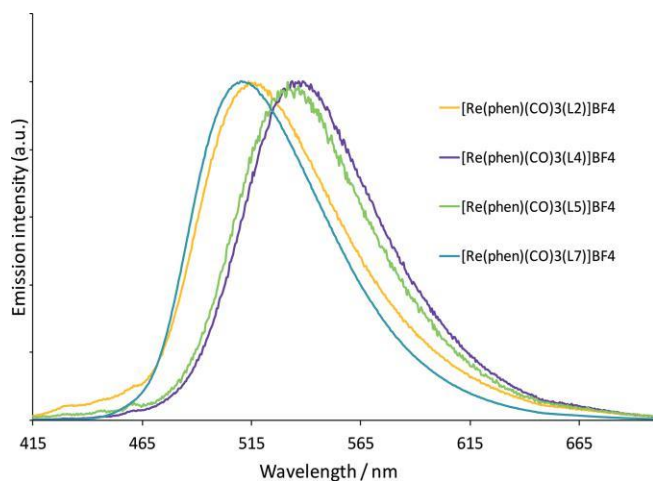

Figure 6. Comparison of the normalised emission spectra (λ_{exc} = 405 nm) of selected complexes.

[Re(phen)(CO)$_3$(L6)]BF$_4$ and fac-[Re(phen)(CO)$_3$(L7)]BF$_4$, the obtained lifetimes closely match those for the free ligands, suggesting 1,8-naphthalimide-dominated fluorescence emission for those species (Figure 6).

Preliminary Confocal Fluorescence Microscopy Imaging with Fission Yeast

The calculated[20] water/octanol partition coefficients (log P$_{calc}$) were obtained for the free ligands showing that hydrophobicity increased across the series, L1(log P$_{calc}$ = 2.42) < L2(2.99) < L3(3.05) < L4(3.33) < L5(3.38) < L6(3.57) < L7(3.62). These values predicted that addition of either piperidine or benzylamine substituents led to the most hydrophobic derivatives; enhanced lipophilicity is a common strategy for encouraging cellular uptake of a given agent. Preliminary confocal fluorescence microscopy was conducted on a selection of complexes to assess their prospective imaging capabilities. Complexes were incubated with fission yeast cells (*Schizosaccharomyces pombe*). Yeast cell walls typically allow translocation of compounds with molecular weights <1000 Da and were thus deemed suitable species for probing the fluorophores described herein. Cells were imaged by using λ_{exc} = 405 nm and a detection wavelength window of 500–600 nm. Imaging was initially conducted with the 3-picolyl variants fac-[Re(phen)(CO)$_3$(L)]BF$_4$ species (where L = L1, L3, L4, L5 and L7). Cells were incubated with the complexes at a concentration of 10 µg per mL, but resulted in very poor observed uptake. An increased probe concentration of 100 µg per mL generally resulted in much better uptake, although for fac-[Re(phen)(CO)$_3$(L3)]BF$_4$ uptake remained poor (only a handful of cells were stained), and both fac-[Re(phen)(CO)$_3$(L4)]BF$_4$ and fac-[Re(phen)(CO)$_3$(L5)]BF$_4$ showed evidence of precipitate formation at these higher concentrations. Even though uptake for fac-[Re(phen)(CO)$_3$(L1)]BF$_4$

(where emission was dominated by $^3M_{Re}L_{phen}CT$) was judged to be relatively modest, good quality cell images were still obtained (Figure 7) showing uptake in both individual and dividing cells. These general observations for limiting uptake has been noted previously in yeast imaging work with other Re^I–diimine complexes incorporating various axial ligands (including those adorned with alkyl chains) that impart significantly greater lipophilicity than the complexes discussed herein.[21] In those cases a 100 µg per mL luminophore concentration was also used for the cell incubation work and the complexes were observed to be relatively non-toxic with minimal photobleaching.

Of the complexes investigated in these bioimaging studies, the most lipophilic benzylamine-substituted complex fac-[Re(phen)(CO)$_3$(L7)]BF$_4$ showed the best uptake (Figure 8). Even at 10 µg per mL incubation concentration, it showed some cytoplasmic staining and putative mitochondrial accumulation. At the higher incubation concentration, remarkably detailed images were collected that showed clear concentration of the compound in nuclei, particularly in dividing cells where two nuclei were present; cell division weakens the wall and membranes, enhancing their permeability and allowing uptake of the fluorophore.[21]
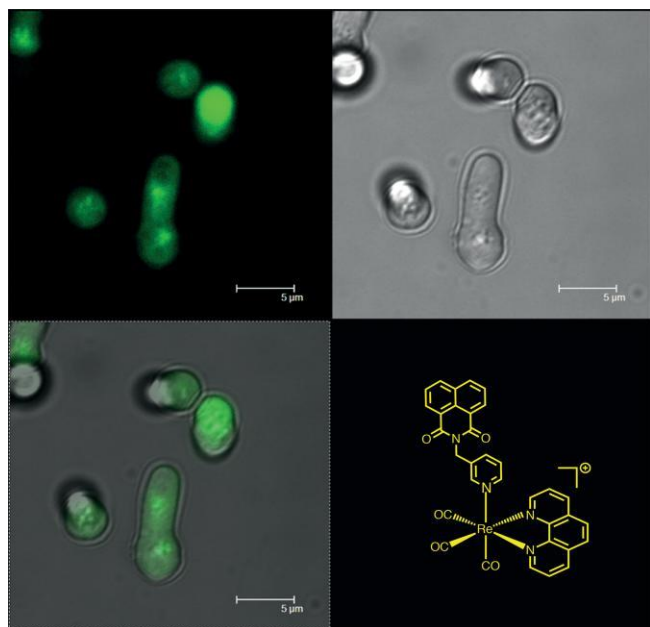
Figure 7. Confocal fluorescence microscopy of *S. pombe* yeast cells incubated with *fac*-[Re(phen)(CO)3(**L1**)]BF4 (λ_{exc} = 405 nm; λ_{em} = 500–600 nm) depicted in green; greyscale shows corresponding Nomarski D.I.C. transmitted light image. Scalebar in microns.

Figure 8. Confocal fluorescence microscopy of *S. pombe* yeast cells incubated with *fac*-[Re(phen)(CO)3(**L7**)]BF4 (λ_{exc} = 405 nm; λ_{em} = 500–600 nm) depicted in green; greyscale shows corresponding N omarski D.I.C. transmitted light image. Scalebar in microns.
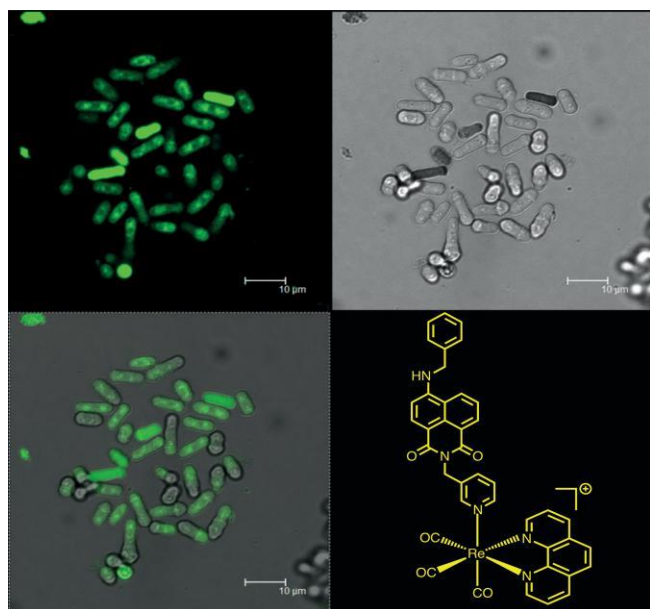
Throughout the duration of the imaging experiments the populations of the cells were monitored with respect to an un-stained control population. For *fac*-[Re(phen)(CO)3(**L1**)]BF4 the cell populations showed a very good stability perhaps reflecting the relatively poor uptake of this agent, whereas cells incubated with *fac*-[Re(phen)(CO)3(**L7**)]BF4 showed a 47 % drop in popula-tion after 4 h. Both complexes also showed a degree of photo-

bleaching which should be noted in future studies and may infer some phototoxicity.

Conclusions

Picolyl-derived ligands can be adorned with a range of naphthalimide derivatives to yield fluorescent species with tuneable emission. These ligands coordinate with Re[I] to give mixed ligand species of the form *fac*-[Re(phen)(CO)3(L)]BF4. The resultant complexes were characterised by using a range of spectroscopic techniques, and all were found to be lumines-cent. The origin of the luminescence, be it $^3M_{ReL_{phen}}CT$ or li-gand-based, varies according to the nature of the specific naphthalimide ligand. A selection of complexes were chosen for cell imaging studies with fission yeast cells (*S. pombe*), and two examples were shown to be viable cell imaging agents. Uptake of the complexes appears to be modulated by the na-ture of the naphthalimide functionalisation, with the most lipo-philic variant showing the best cell uptake.

Experimental Section

X-ray Crystallography: Suitable crystals were selected and meas-ured following a standard method[22] on a *Rigaku AFC12* goniome-ter equipped with an enhanced sensitivity (HG) *Saturn724+* detector mounted at the window of a *FR-E+ SuperBright* molybdenum rotat-ing anode generator with VHF *Varimax* optics (70 µm focus) at 100 K. Cell determination, data collection, reduction, cell refinement and absorption correction carried out by using *CrystalClear-SM Ex-pert 3.1b27*.[23]

By using Olex2,[24] the structure was solved by charge flipping using *SUPERFLIP*[25] and the models were refined with version 2014/7 of ShelXL[26] using Least Squares minimisation. All non-H atoms were refined anisotropically and difference Fourier syntheses were em-ployed in positioning idealised hydrogen atoms and were allowed to ride on their parent C-atoms. It was not possible to accurately model the highly disordered solvent and thus PLATON SQUEEZE[27] was used. Disorder in most of the BF4 anions, resulting in both geometrical (SAME, BUMP) and displacement (RIGU, SIMU) restraints been employed.

Cell Incubation and Confocal Microscopy: The fission yeast *Schizosaccharomyces pombe* 972 h- was grown in 20 mL of medium containing glucose (1 %), peptone (1 %), and yeast extract (0.3 %) in Ehrlenmeyer flasks shaken at 30 °C for 2 d, when glucose utilisa-tion was complete. Washed once in PBS (phosphate-buffered saline, pH 7.4) after centrifugation at 1000 g for 2 min, they were incubated for 30 min with fluorophores in DMSO with PBS buffer at 10 and 100 µg per mL (final concentrations in growth medium) at 20 °C before washing again in PBS. Preparations were viewed by epifluo-rescence and transmitted light (Nomarski differential interference contrast optics) by using a Leica TCS SP2 AOBS confocal laser scan-ning microscope (Leica, Germany) using ×63 or ×100 objectives, ×4 zoom factor and laser power of 20 %. Excitation of the fluorophore was at 405 nm by using a 20 mW diode laser, with detection be-tween 500–600 nm. In the majority of cases, initial imaging yielded minimal detectable fluorescence so the concentration of the fluoro-phore was increased to 100 µg per mL final concentration, which was then incubated with the cells at room temperature for a further 30 min.

General: ^{1}H and ^{13}C{^{1}H} NMR spectra were recorded on an NMR-FT Bruker 400 and 250 MHz spectrometer and recorded in CDCl3. ^{1}H and ^{13}C{^{1}H} NMR chemical shifts (δ) were determined relative to residual solvent peaks with digital locking and are given in ppm. Low-resolution mass spectra were obtained by the staff at Cardiff University. High-resolution mass spectra were carried out at the EPSRC National Mass Spectrometry Facility at Swansea University. UV/Vis studies were performed on a Jasco V-570 spectrophotometer as MeCN solutions (2.5 or 5×10^{-5} M). Photophysical data were ob-tained on a JobinYvon–Horiba Fluorolog spectrometer fitted with a JY TBX picosecond photodetection module as MeCN solutions. Emission spectra were uncorrected and excitation spectra were in-strument corrected. The pulsed source was a Nano-LED configured for 459 nm output operating at 1 MHz. Luminescence lifetime pro-files were obtained by using the JobinYvon–Horiba FluoroHub sin-gle photon counting module and the data fits yielded the lifetime values by using the provided DAS6 deconvolution software.

All reactions were performed with the use of vacuum line and Schlenk techniques. Reagents were commercial grade and used without further purification. N-(4′-Picolylamine)-1,8-naphthalimide (**L1**)[28] and fac-[Re(phen)(CO)3(MeCN)]BF4[29] were prepared accord-ing to the literature.

Synthesis

Synthesis of 4-Chloro-N-(4′-picolylamine)-1,8-naphthalimide (L2): Prepared as for **L1** but with 4-chloro-1,8-naphthalic anhydride (1.997 g, 8.58 mmol) and 4-picolylamine (1.75 mL, 17.2 mmol) to give **L2** as a yellow solid (yield: 2.216 g, 80 %). ^{1}H NMR (250 MHz, CDCl3): δ_H = 8.71–8.48 (m, 5 H), 7.93–7.78 (m, 2 H), 7.39 (d, $^3J_{HH}$ = 5.7 Hz, 2 H), 5.37 (s, 2 H, CH2) ppm. UV/Vis (CH3CN): λ_{max} (ε/M^{-1} cm^{-1}) = 353 (10800), 340 (12600), 235 (36300), 210 (20100) nm.

Synthesis of 4-Chloro-N-(3′-picolylamine)-1,8-naphthalimide (L3): Prepared as for **L1** but with 4-chloro-1,8-naphthalic anhydride (1.975 g, 8.49 mmol) and 3-picolylamine (1.75 mL, 17.2 mmol) to give **L3** as a yellow solid (yield: 2.444 g, 89 %). ^{1}H NMR (250 MHz, CDCl3): δ_H = 8.76 (d, $^3J_{HH}$ = 1.4 Hz, 1 H), 8.62–8.37 (m, 4 H), 7.86–7.70 (m, 3 H), 7.21–7.13 (m, 1 H), 5.30 (s, 2 H, CH2) ppm. ^{13}C{^{1}H} NMR (300 MHz, CDCl3): δ_C = 163.7 (CO), 163.5 (CO), 150.7, 149.0, 139.5, 137.1, 132.8, 132.4, 131.5, 131.0, 129.4, 127.9, 127.5, 123.5, 122.8, 121.3, 41.3 (CH2) ppm. LRMS (ES$^+$) found m/z 323.06 for [M + H]$^+$, calculated 323.73 for [M + H]$^+$. HRMS (ES$^+$) found m/z = 323.0583, calculated 323.0582 for [C18H12N2O2Cl]$^+$. IR (solid): $\tilde{v}_{max}$ = 1697 (C=O), 1655 (C=O), 1616, 1590, 1570, 1505, 1478, 1462, 1400, 1373, 1339, 1316, 1234, 1225, 1173, 1159, 1117, 1094, 1053, 1028, 995, 955, 934, 912, 851, 793, 777 (C–Cl), 752, 733, 714, 667, 623 cm^{-1}. UV/Vis (CH3CN): λ_{max} (ε/M^{-1} cm^{-1}) = 353 (13400), 340 (15600), 235 (52100) nm.

Synthesis of 4-Piperidyl-N-(4′-picolylamine)-1,8-naphthalimide (L4): **L2** (104 mg, 0.32 mmol) and piperidine (0.13 mL, 1.29 mmol) were heated in DMSO (6 mL) under a dinitrogen atmosphere at 80 °C for 2 h. The solution was cooled and then water was added to induce precipitation of the product upon neutralisation with 1 M HCl. The solution was then filtered and the solid washed with copi-ous amounts of water, followed by petroleum ether, and subse-quently dried in vacuo to give **L4** as a yellow solid (yield: 86 mg, 72 %). ^{1}H NMR (400 MHz, CDCl3): δ_H = 8.52 (d, $^3J_{HH}$ = 7.3 Hz, 1 H), 8.38–8.49 (m, 3 H), 8.34 (d, $^3J_{HH}$ = 8.4 Hz, 1 H), 7.68 (app t, $^3J_{HH}$ = 7.3 Hz, 2 H), 7.63 (dd, J_{HH} = 8.4, 8.5 Hz, 1 H), 7.32 (d, $^3J_{HH}$ = 5.9 Hz, 2 H), 7.12 (d, $^3J_{HH}$ = 8.2 Hz, 1 H), 5.30 (s, 2 H, CH2), 3.18 (t, $^3J_{HH}$ = 5.0 Hz, 4 H, CH2), 1.87–1.72 (m, 4 H, NCH2CH2) ppm. UV/Vis (CH3CN): λ_{max} (ε/M^{-1} cm^{-1}) = 411 (10400), 339 (2000), 326 (1900), 275 (16000), 260 (17900), 225 (25000), 207 (33100) nm.

Synthesis of 4-Piperidyl-N-(3′-picolylamine)-1,8-naphthalimide (L5): Prepared as for **L4** with **L3** (100 mg, 0.31 mmol) and piperidine (0.06 mL, 0.62 mmol) however in this instance isolation of the pure product resulted from extraction of the neutralised reaction mixture into dichloromethane (2 × 20 mL). The organic layer was washed with water (3 × 20 mL), dried with MgSO4 and reduced to a mini-mum volume. Precipitation of the product was then induced via the slow addition of petroleum ether. Subsequent filtration and dry-ing in vacuo gave **L5** as an orange solid (yield: 111 mg, 98 %). ^{1}H NMR (400 MHz, CDCl3): δ_H = 8.81 (s, 1 H), 8.53–8.47 (m, 2 H), 8.43 (d, $^3J_{HH}$ = 8.2 Hz, 1 H), 8.34 (d, $^3J_{HH}$ = 8.4 Hz, 1 H), 8.19 (broad d, $^3J_{HH}$ = 7.9 Hz, 1 H), 7.63 (dd, J_{HH} = 7.4, 7.3 Hz, 1 H), 7.49–7.42 (m, 1 H), 7.12 (d, $^3J_{HH}$ = 8.2 Hz, 1 H), 5.37 (s, 1 H, CH2), 3.19 (t, $^3J_{HH}$ = 5.1 Hz, 4 H, CH2), 1.88–1.79 (m, 4 H, CH2CH2), 1.72–1.64 (m, 2 H) ppm. ^{13}C{^{1}H} NMR (300 MHz, CDCl3): δ_C = 164.6 (CO), 164.0 (CO), 157.7, 150.6, 148.8, 136.9, 133.3, 133.1, 131.4, 131.1, 130.0, 126.2, 125.4, 123.4, 122.8, 115.4, 114.8, 54.6, 41.0 (CH2), 26.2, 24.3 ppm. LRMS (ES$^+$) found m/z = 372.17 for [M + H]$^+$. HRMS (ES$^+$) found m/z = 372.1706, calculated 372.1707 for [C23H22N2O2]$^+$. IR (solid): $\tilde{v}_{max}$ = 1688 (C=O), 1645 (C=O), 1584, 1570, 1512, 1481, 1449, 1429, 1414, 1377 (C–N), 1350, 1339, 1316, 1277, 1250, 1231, 1219, 1192, 1175, 1153, 1124, 1105, 1076, 1039, 1028, 985, 958, 939, 897, 864, 843, 814, 779, 758, 741, 712, 665 cm^{-1}. UV/Vis (CH3CN): λ_{max} (ε/M^{-1} cm^{-1}) = 410 (10800), 340 (2500), 325 (2300), 259 (15900), 224 (24800), 209 (34600) nm.

Synthesis of 4-Benzylamine-N-(4-picolylamine)-1,8-naphthal-imide (L6): Prepared as for **L5** but with **L2** (101 mg, 0.31 mmol) and benzylamine (0.10 mL, 0.62 mmol) in DMSO (4 mL), heating for 12 h to give **L6** as a yellow–orange solid which was recrystallised from MeOH/ice cooled petroleum ether (yield: 122 mg, 94 %). ^{1}H NMR (400 MHz, CDCl3): δ_H = 8.62 (d, $^3J_{HH}$ = 7.3 Hz, 1 H), 8.52 (d, $^3J_{HH}$ = 5.7 Hz, 1 H), 8.48 (d, $^3J_{HH}$ = 8.4 Hz, 1 H), 8.17 (d, $^3J_{HH}$ = 8.5 Hz, 1 H), 7.66 (app. t, 1 H), 7.55–7.33 (m, 7 H), 6.80 (d, $^3J_{HH}$ = 8.5 Hz, 1 H), 5.68 (t, $^3J_{HH}$ = 5.2 Hz, 1 H, NH), 5.38 (s, 2 H, CH2), 4.64 (d, $^3J_{HH}$ = 5.1 Hz, 2 H, CH2) ppm. ^{13}C{^{1}H} NMR (300 MHz, CDCl3): δ_C = 164.6 (CO), 164.0 (CO), 149.8, 149.6, 146.8, 137.0, 135.0, 131.7, 130.4, 130.0, 129.2, 128.2, 127.7, 126.6, 125.1, 123.3, 122.7, 120.4, 110.3, 105.2, 48.1 (NHCH2), 42.5 (CH2) ppm. LRMS (ES$^+$) found m/z = 394.11 for [M + H]$^+$. HRMS (ES$^+$) found m/z = 394.1548, calculated 394.1550 for [C25H20O2N3]$^+$. IR (solid): $\tilde{v}_{max}$ = 3300 (N–H), 1684 (C=O), 1643 (C=O), 1574 (N–H bend), 1539, 1495, 1451, 1416, 1387, 1370, 1341, 1314, 1295, 1242, 1182, 1163, 1130, 1098, 1067, 1028, 991, 979, 963, 939, 772, 758, 737, 696, 669, 652, 633 cm^{-1}. UV/Vis (CH3CN): λ_{max} (ε/M^{-1} cm^{-1}) = 429 (8100), 353 (3300), 339 (3800), 325 (3200), 279 (11600), 256 (11600), 229 (16100), 202 (36900) nm.

Synthesis of 4-Benzylamine-(N-3-picolylamine)-1,8-naphthal-imide (L7): Prepared as for **L6** but with **L3** (174 mg, 0.54 mmol) and benzylamine (0.24 mL, 2.16 mmol) to give **L7** as an orange solid (yield: 90 mg, 42 %) ^{1}H NMR (400 MHz, CDCl3): δ_H = 8.74 (s, 1 H), 8.52 (d, $^3J_{HH}$ = 8.0 Hz, 1 H), 8.36–8.42 (m, 2 H), 8.06 (d, $^3J_{HH}$ = 8.5 Hz, 1 H), 7.84–7.78 (m, 1 H), 7.53 (dd, J_{HH} = 7.5, 7.3 Hz, 1 H), 7.39–7.24 (m, 5 H), 7.18–7.11 (m, 1 H), 6.68 (d, $^3J_{HH}$ = 8.5 Hz, 1 H), 5.69 (t, $^3J_{HH}$ = 4.8 Hz, 1 H, NH), 5.29 (s, 2 H, CH2), 4.54 (d, $^3J_{HH}$ = 5.1 Hz, 2 H, CH2) ppm. ^{13}C{^{1}H} NMR (300 MHz, CDCl3): δ_C = 164.7 (CO), 164.0 (CO), 150.6, 149.5, 148.7, 136.9, 136.9, 134.9, 133.6, 131.6, 129.8, 129.2, 128.2, 127.7, 126.5, 125.0, 123.5, 122.9, 120.4, 110.4, 105.1, 48.1 (NHCH2), 41.0 (CH2) ppm. LRMS (ES$^+$) found m/z = 394.16 for [M + H]$^+$. HRMS (ES$^+$) found m/z = 394.1150, calculated 394.1150 for [C25H20N3O2]$^+$. IR (solid): $\tilde{v}_{max}$ = 3350 (N–H), 1734, 1674 (C=O), 1630 (C=O), 1614, 1576 (N–H bend), 1559, 1516, 1497, 1479, 1451, 1429, 1393, 1369, 1344, 1318, 1298, 1236, 1221, 1186, 1163, 1132, 1120, 1103, 1096, 1065, 1043, 1030, 988, 970, 932, 856, 843, 816, 801, 769, 754, 714, 702, 669, 663 cm^{-1}. UV/Vis (CH3CN): λ_{max}

$(\varepsilon/\text{M}^{-1}\ \text{cm}^{-1})$ = 428 (12000), 356 (2100), 339 (2400), 324 (2300), 279 (17100), 258 (16400), 227 (16400), 202 (44000) nm.

Synthesis of *fac*-[Re(phen)(CO)₃(L1)]BF₄: *fac*-[Re(phen)(CO)₃(MeCN)]BF₄ (47 mg, 80.8 µmol) and **L1** (26 mg, 88.9 µmol) were dissolved in chloroform (3 mL) and heated at reflux, under a dinitrogen atmosphere, for 12 h. After cooling the solvent was reduced in vacuo. Precipitation of the product was then induced via the slow addition of diethyl ether. The product was subsequently filtered and dried in vacuo to give the product as an off-white solid (yield: 60.3 mg, 90 %). ¹H NMR (400 MHz, CD₃CN): δ_H = 9.45 (dd, J_{HH} = 5.4, 5.1 Hz, 2 H), 8.92 (dd, J_{HH} = 8.3, 7.8 Hz, 2 H), 8.76–8.73 (m, 1 H), 8.60 (d, ³J_{HH} = 7.3 Hz, 2 H), 8.46 (d, ³J_{HH} = 5.3 Hz, 1 H), 8.40 (d, ³J_{HH} = 8.2 Hz, 2 H), 8.28 (s, 2 H), 8.10 (dd, J_{HH} = 8.3, 5.1 Hz, 2 H), 7.94–7.90 (m, 1 H), 7.86 (app. t, 2 H), 7.38 (dd, J_{HH} = 8.2, 4.8 Hz, 1 H), 5.36 (s, 2 H, CH_2) ppm. ¹³C{¹H} NMR (300 MHz, CD₃CN): very weak δ_C = 205.4 (M—CO), 161.5 (NCCO), 161.3 (NCCO), 154.6, 152.8, 150.2, 148.9, 140.1, 136.6, 134.5, 131.1, 128.0, 127.2, 125.6, 87.8 (CH₂) ppm. LRMS (ES⁺) found m/z = 737.10 for [M]⁺. HRMS (ES⁺) found m/z = 737.0953, calculated 737.0598 for [C₃₃H₂₀N₄O₅Re]⁺. IR (solid): $\tilde{\nu}_{max}$ = (selected) = 2029 (C≡O), 1950 (C≡O), 1907 (C≡O), 1694 (C=O), 1655 (C=O), 1060 (BF₄) cm⁻¹. UV/Vis (CH₃CN): λ_{max} ($\varepsilon/\text{M}^{-1}$ cm⁻¹) = 345 (14100), 332 (15900), 273 (43000), 230 (61600), 210 (46200), 202 (48200) nm.

Synthesis of *fac*-[Re(phen)(CO)₃(L2)]BF₄: Prepared as for *fac*-[Re(phen)(CO₃)(L1)]BF₄ with *fac*-[Re(phen)(CO)₃(MeCN)]BF₄ (31 mg, 53.6 µmol) and **L2** (19 mg, 59.0 µmol) to give *fac*-[Re(phen)(CO₃)(L2)]BF₄ as a yellow solid (yield: 31 mg, 68 %). ¹H NMR (400 MHz, CDCl₃): δ_H = 9.46 (dd, J_{HH} = 5.1, 3.8 Hz, 2 H), 8.67 (d, ³J_{HH} = 7.6 Hz, 2 H), 8.43 (d, ³J_{HH} = 8.5 Hz, 1 H), 8.33 (d, ³J_{HH} = 7.2 Hz, 1 H), 8.17 (d, ³J_{HH} = 7.9 Hz, 1 H), 8.12–8.06 (m, 2 H), 7.97 (s, 2 H), 8.00–7.92 (m, 2 H), 7.74–7.69 (m, 2 H), 7.09 (d, ³J_{HH} = 6.6 Hz, 2 H), 4.99 (s, 2 H, CH_2) ppm. ¹³C{¹H} NMR (300 MHz, CD₃CN): δ_C = 163.4 (CO), 163.2 (CO), 154.5, 151.9, 150.8, 146.6, 140.3, 140.2, 138.8, 131.9, 131.3, 131.1, 130.8, 129.0, 128.8, 128.3, 128.1, 127.6, 127.1, 125.5, 122.6, 121.3, 118.2, 78.2, 42.1 (CH₂) ppm. LRMS (ES⁺) found m/z = 773.21 for [M]⁺. HRMS (FTMS) found m/z = 771.0567, calcu-lated 771.0568 for [ReC₃₃H₁₉N₄O₅Cl]⁺. IR (solid): $\tilde{\nu}_{max}$ = (selected) = 2023 (C≡O), 1903 (C≡O), 1697 (C=O), 1654 (C=O), 1047 (BF₄) cm⁻¹. UV/Vis (CH₃CN): λ_{max} ($\varepsilon/\text{M}^{-1}$ cm⁻¹) = 353 (16600), 340 (19700), 327 (17200), 274 (37000), 231 (67200), 213 (66400) nm.

Synthesis of *fac*-[Re(phen)(CO)₃(L3)]BF₄: Prepared as for *fac*-[Re(phen)(CO₃)(L1)]BF₄ but with *fac*-[Re(phen)(CO)₃(MeCN)]BF₄ (38 mg, 65.9 µmol) and **L3** (25 mg, 73.2 µmol) to give *fac*-[Re(phen)(CO₃)(L3)]BF₄ as a yellow solid (yield: 46 mg, 82 %). ¹H NMR (400 MHz, CD₃CN): δ_H = 9.42 (d, ³J_{HH} = 3.6 Hz, 2 H), 8.59–8.50 (m, 3 H), 8.35 (dd, J_{HH} = 7.3, 1.0 Hz, 1 H), 8.26 (d, ³J_{HH} = 5.6 Hz, 1 H), 8.20 (d, ³J_{HH} = 7.9 Hz, 2 H), 8.01 (d, ³J_{HH} = 1.6 Hz, 1 H), 7.92–7.81 (m, 7 H), 7.07 (dd, J_{HH} = 7.8, 5.7 Hz, 1 H), 4.83 (s, 2 H, CH_2) ppm. ¹³C{¹H} NMR (300 MHz, CD₃CN): δ_C = 195.7 (C≡O), 191.2 (C≡O), 163.2 (CO), 163.0 (CO), 154.5, 154.4, 152.0, 151.7, 146.5, 140.8, 140.2, 138.9, 136.0, 132.0, 131.2, 130.8, 129.1, 128.8, 128.4, 128.0, 127.7, 127.1, 126.2, 122.6, 121.3, 40.3 (CH₂) ppm. LRMS (ES⁺) found m/z = 773.12 for [M]⁺. HRMS (ES⁺) found m/z = 771.0570, calculated 771.0568 for [C₃₃H₁₉O₅N₄ClRe]⁺. IR (solid): $\tilde{\nu}_{max}$ = (selected) = 2027 (C≡O), 1928 (C≡O), 1911 (C≡O), 1701 (C=O), 1666 (C=O), 1053 (BF₄) cm⁻¹. UV/Vis (CH₃CN): λ_{max} ($\varepsilon/\text{M}^{-1}$ cm⁻¹) = 354 (16700), 340 (19600), 326 (17100), 274 (32200), 233 (62300), 211 (61000) nm.

Synthesis of *fac*-[Re(phen)(CO)₃(L4)]BF₄: Prepared as for *fac*-[Re(phen)(CO₃)(L1)]BF₄ with *fac*-[Re(phen)(CO)₃(MeCN)]BF₄ (40 mg, 69.2 µmol) and **L4** (28 mg, 76.1 µmol) to give the product as an orange–yellow solid (yield: 42 mg, 67 %). ¹H NMR (400 MHz, CDCl₃): δ_H = 9.50 (d, ³J_{HH} = 4.6 Hz, 2 H), 8.77 (d, ³J_{HH} = 8.1 Hz, 2 H), 8.34

(d, ³J_{HH} = 6.6 Hz, 1 H), 8.28 (app. t, 2 H), 8.28–8.16 (m, 6 H), 7.55 (app. t, 1 H), 7.17 (d, ³J_{HH} = 6.3 Hz, 2 H), 7.04 (d, ³J_{HH} = 8.2 Hz, 1 H), 5.09 (s, 2 H, CH_2), 3.15 (t, ³J_{HH} = 4.6 Hz, 4 H, CH_2), 1.86–1.78 (m, 4 H, CH_2), 1.71–1.60 (m, 2 H, CH_2) ppm. ¹³C{¹H} NMR (300 MHz, CDCl₃): δ_C = 195.1 (C≡O), 164.3 (CO), 163.7 (CO), 158.1, 154.3, 153.9, 152.0, 151.5, 151.3, 146.4, 140.6, 140.6, 133.4, 131.6, 131.4, 130.1, 128.6, 127.7, 126.1, 125.7, 125.4, 122.1, 114.8, 144.4, 52.5, 42.0, 26.1, 24.3 ppm. LRMS (ES⁺) found m/z = 822.20 for [M]⁺. HRMS (ES⁺) found m/z = 820.1690, calculated 820.1693 for [C₃₈H₂₉N₅O₅Re]⁺. IR (solid): $\tilde{\nu}_{max}$ = (selected) = 2029 (C≡O), 1911 (C≡O), 1691, (C=O), 1654 (C=O), 1051 (BF₄) cm⁻¹. UV/Vis (CH₃CN): λ_{max} ($\varepsilon/\text{M}^{-1}$ cm⁻¹) = 408 (9700), 340 (5600), 326 (6600), 274 (36700) nm.

Synthesis of *fac*-[Re(phen)(CO)₃(L5)]BF₄: Prepared as for *fac*-[Re(phen)(CO₃)(L1)]BF₄ with *fac*-[Re(phen)(CO)₃(MeCN)]BF₄ (39 mg, 67.4 µmol) and **L5** (31 mg, 74.1 µmol) to give the product as an orange solid (yield: 39 mg, 64 %). ¹H NMR (400 MHz, CDCl₃): δ_H = 9.54 (d, ³J_{HH} = 4.6 Hz, 2 H), 8.82–8.76 (m, 2 H), 8.42–8.36 (m, 3 H), 8.33 (d, ³J_{HH} = 7.9 Hz, 2 H), 8.10–8.01 (m, 5 H), 7.96 (d, ³J_{HH} = 7.9 Hz, 1 H), 7.73 (app. t, 1 H), 5.02 (s, 2 H, CH_2), 3.27 (broad t, 4 H, CH_2), 1.94–1.86 (m, 4 H, CH_2), 1.80–1.79 (m, 2 H, CH_2) ppm. ¹³C{¹H} NMR (300 MHz, CDCl₃): δ_C = 195.3 (C≡O), 164.1 (C=O), 153.6, 153.1, 152.5, 152.3, 151.4, 146.3, 141.2, 140.6, 133.3, 131.8, 131.8, 131.4, 131.4, 128.6, 128.1, 127.5, 127.3, 126.9, 125.8, 125.7, 122.1, 54.8, 54.5, 40.0, 26.0, 24.1 ppm. LRMS (ES⁺) found m/z = 822.24 for [M]⁺. HRMS (ES⁺) found m/z = 820.1691, calculated 820.1693 for [C₃₈H₂₉N₅O₅Re]⁺. IR (solid): $\tilde{\nu}_{max}$ = (selected) = 2031 (C≡O), 1911 (C≡O), 1691 (C=O), 1651 (C=O), 1057 (BF₄) cm⁻¹. UV/Vis (CH₃CN): λ_{max} ($\varepsilon/\text{M}^{-1}$ cm⁻¹) = 406 (7000), 274 (34500) nm.

Synthesis of *fac*-[Re(phen)(CO)₃(L6)]BF₄: Prepared as for *fac*-[Re(phen)(CO₃)(L1)]BF₄ but with *fac*-[Re(phen)(CO)₃(MeCN)]BF₄ (38 mg, 65.7 µmol) and **L6** (27 mg, 72.3 µmol) to give the product as a yellow solid (yield: 42 mg, 61 %). ¹H NMR (250 MHz, CD₃CN): δ_H = 9.60 (d, ³J_{HH} = 5.13 Hz, 2 H), 8.81 (dd, J_{HH} = 7.6, 7.9 Hz, 2 H), 8.40 (app. t, 2 H), 8.24–8.06 (m, 8 H), 7.65 (t, ³J_{HH} = 8.1 Hz, 1 H), 7.51–7.32 (m, 4 H), 7.18 (d, ³J_{HH} = 7.4 Hz, 2 H), 6.98 (t, 1 H, J = 5.3 Hz, NH), 6.62 (d, ³J_{HH} = 8.0 Hz, 1 H), 5.10 (s, 2 H, CH_2), 4.68 (d, ³J_{HH} = 6.0 Hz, 2 H, CH_2) ppm. ¹³C{¹H} NMR (300 MHz, CD₃CN): δ_C = 195.5 (C≡O), 191.5 (C≡O), 164.2 (C=O), 163.1 (C=O), 154.7, 151.7, 150.3, 146.6, 140.3, 138.2, 134.1, 131.3, 131.0, 128.7, 128.1, 127.9, 127.4, 127.2, 127.1, 125.4, 124.7, 122.1, 120.3, 108.8, 104.8, 46.43 (CH₂), 41.6 (NHCH₂) ppm. LRMS (ES⁺) found m/z = 844.24 for [M]⁺. HRMS found m/z = 842.1536, calculated 842.1536 for [C₄₀H₂₇N₅O₅Re]⁺. IR (solid): $\tilde{\nu}_{max}$ = (selected) = 2031 (C≡O), 1913 (C≡O), 1685 (C=O), 1647 (C=O), 1053 (BF₄) cm⁻¹. UV/Vis (CH₃CN): λ_{max} ($\varepsilon/\text{M}^{-1}$ cm⁻¹) = 431 (14600), 354 (6900), 337 (9300), 323 (9600), 275 (47300), 256 (39800), 226 (58400) nm.

Synthesis of *fac*-[Re(phen)(CO)₃(L7)]BF₄: Prepared as for *fac*-[Re(phen)(CO₃)(L1)]BF₄ but with *fac*-[Re(phen)(CO)₃(MeCN)]BF₄ (42 mg, 72.1 µmol) and **L7** (31 mg, 79.3 µmol) to give the product as a yellow solid (yield: 43 mg, 64 %). ¹H NMR (400 MHz, CD₃CN): δ_H = 9.39 (d, ³J_{HH} = 3.8 Hz, 2 H), 8.44 (m, 2 H), 8.32 (d, ³J_{HH} = 4.9 Hz, 2 H), 8.29 (d, ³J_{HH} = 8.2 Hz, 2 H), 8.02 (d, ³J_{HH} = 8.6 Hz, 1 H), 7.83 (s, 1 H), 7.82–7.71 (m, 5 H), 7.66 (app. t, 1 H), 7.51 (s, 1 H), 7.41 (d, ³J_{HH} = 7.5 Hz, 2 H), 7.31 (app. t, 2 H), 7.11 (dd, J_{HH} = 7.7, 5.6 Hz, 1 H), 7.02 (app s, 1 H, NH), 6.66 (d, ³J_{HH} = 8.6 Hz, 1 H), 4.83 (s, 2 H, CH_2), 4.66 (d, ³J_{HH} = 6.0 Hz, 2 H, CH_2) ppm. ¹³C{¹H} NMR (300 MHz, CD₃CN): δ_C = 195.7 (C≡O), 191.5 (C≡O), 163.8 (C=O), 162.9 (C=O), 154.3, 151.7, 150.5, 146.3, 140.3, 139.9, 140.0, 138.3, 137.0, 134.3, 131.2, 131.0, 129.7, 128.7, 128.0, 127.8, 127.4, 127.3, 126.9, 126.1, 124.9, 122.1, 120.7, 120.6, 119.9, 119.1, 105.0, 46.5 (CH₂), 39.9 (NHCH₂) ppm. LRMS (ES⁺) found m/z = 844.16 for [M]⁺. HRMS (FTMS) found m/z 842.1543 for [C₄₀H₂₇N₅O₅Re]⁺, calculated

Acknowledgments

[1] For example, N. I. Georgiev, V. B. Bojinov, M. Marinova, *Sens. Actuators B* **2010**, *150*, 655; N. I. Georgiev, V. B. Bojinov, *Dyes Pigm.* **2010**, *84*, 249; V. B. Bojinov, N. I. Georgiev, P. S. Nikolov, *J. Photochem. Photobiol. A* **2008**, *197*, 281; A. M. M. El-Betany, L. Vachova, C. G. Bezzu, S. J. A. Pope, N. B. McKeown, *Tetrahedron* **2013**, *69*, 8439; C. Felip-Leon, S. Diaz-Oltra, F. Gal-indo, J. F. Miravet, *Chem. Mater.* **2016**, *28*, 7964; R. K. Dubey, D. Inan, S. Sengupta, E. J. R. Sudholter, F. C. Grozema, W. F. Jager, *Chem. Sci.* **2016**, *7*, 3517; C.-C. You, C. Hippius, M. Grüne, F. Würthner, *Chem. Eur. J.* **2006**, *12*, 7510.

[2] R. M. Duke, E. B. Veale, F. M. Pfeffer, P. E. Kruger, T. Gunnlaugsson, *Chem. Soc. Rev.* **2010**, *39*, 3936.

[3] E. Calatrava, S. A. Bright, S. Achermann, M. O. Senge, E. B. Veale, D. C. Williams, T. Gunnlaugsson, E. M. Scanlan, *Chem. Commun.* **2016**, *52*, 13086; S.-A. Choi, C. S. Park, O. S. Kwon, H.-K. Giong, J.-S. Lee, T. H. Ha, C.-S. Lee, *Sci. Rep.* **2016**, *6*, 26203; C. Satriano, G. T. Sfrazzetto, M. E. Amato, F. P. Ballistreri, A. Copani, M. L. Giuffrida, G. Grasso, A. Pappa-lardo, E. Rizzarelli, G. A. Tomaselli, R. M. Toscano, *Chem. Commun.* **2013**, *49*, 5565; Y. Dai, B.-K. Lv, X.-F. Zhang, Y. Xiao, *Chin. Chem. Lett.* **2014**, *25*, 1001; L. Zhang, F. Su, X. Kong, F. Lee, S. Sher, K. Day, Y. Tian, D. R. Mel-drum, *ChemBioChem* **2016**, *17*, 1719.

[4] M. J. Waring, A. Gonzalez, A. Jimenez, D. Vazquez, *Nucl. Acid Res.* **1979**, *7*, 217; B. S. Andersson, M. Beran, N. Bakic, L. E. Silbermann, R. A. New-man, *Cancer Res.* **1987**, *47*, 1040; K. A. Stevenson, S. F. Yen, N. C. Yang, D. W. Boykin, W. D. Wilson, *J. Med. Chem.* **1984**, *27*, 1677; R. K. Y. Zee-Cheng, C. C. Cheng, *J. Med. Chem.* **1985**, *28*, 1216.

[5] G. Gellerman, *Lett. Drug Des. Discovery* **2016**, *13*, 47.

[6] For example, M. Lv, H. Xu, *Curr. Med. Chem.* **2009**, *16*, 4797; L. Ingrassia, F. Lefranc, R. Kiss, T. Mijatovic, *Curr. Med. Chem.* **2009**, *16*, 1192; Z. Chen, X. Liang, H. Zhang, H. Xie, J. Liu, Y. Xu, W. Zhu, Y. Wang, X. Wang, S. Tan, D. Kuang, X. Qian, *J. Med. Chem.* **2010**, *53*, 2589; A. Wu, Y. Xu, X. Qian, J. Wang, J. Liu, *Eur. J. Med. Chem.* **2009**, *44*, 4674; A. Wu, Y. Xu, X. Qian, *Bioorg. Med. Chem.* **2009**, *17*, 592.

[7] S. Banerjee, E. B. Veale, C. M. Phelan, S. A. Murphy, G. M. Tocci, L. J. Gillespie, D. O. Frimannsson, J. M. Kelly, T. Gunnlaugsson, *Chem. Soc. Rev.* **2013**, *42*, 1601.

[8] S. Tan, K. Han, Q. Li, L. Tong, Y. Yang, Z. Chen, H. Xie, J. Ding, X. Qian, Y. Xu, *Eur. J. Med. Chem.* **2014**, *85*, 207.

[9] D. L. Reger, A. Leitner, M. D. Smith, *Cryst. Growth Des.* **2015**, *15*, 5637.

[10] V. F. Plyusnin, A. S. Kupryakov, V. P. Grivin, A. H. Shelton, I. V. Sazanovich, A. J. H. M. Meijer, J. A. Weinstein, M. D. Ward, *Photochem. Photobiol. Sci.* **2013**, *12*, 1666; A. H. Shelton, I. V. Sazanovich, J. A. Weinstein, M. D. Ward, *Chem. Commun.* **2012**, *48*, 2749.

[11] W. Streciwilk, A. Terenzi, R. Misgeld, C. Frias, P. G. Jones, A. Prokop, B. K. Keppler, I. Ott, *ChemMedChem* **2017**, *12*, 214; J. M. Perez, I. Lopez-Solera, E. I. Montero, M. F. Brana, C. Alonso, S. P. Robinson, C. J. Navarro-Ran-ninger, *J. Med. Chem.* **1999**, *42*, 5482; S. Banerjee, J. A. Kitchen, S. A. Bright, J. E. O'Brien, D. C. Williams, J. M. Kelly, T. Gunnlaugsson, *Chem. Commun.* **2013**, *49*, 8522; C. P. Bagowski, Y. You, H. Scheffler, D. H. Vlecken, D. J. Schmitz, I. Ott, *Dalton Trans.* **2009**, 10799; K. J. Kilpin, C. M. Clavel, F. Edafe, P. J. Dyson, *Organometallics* **2012**, *31*, 7031; J. M. Perez, I. Lopez-Solera, E. I. Montero, M. F. Brana, C. Alonso, S. P. Robinson, C. Navarro-Ranniger, *J. Med. Chem.* **1999**, *42*, 5482; S. Roy, S. Saha, R. Mu-jumdar, R. R. Dighe, A. R. Chakravarty, *Inorg. Chem.* **2009**, *48*, 9501.

[12] E. E. Langdon-Jones, D. Lloyd, A. J. Hayes, S. D. Wainwright, H. J. Mottram, S. J. Coles, P. N. Horton, S. J. A. Pope, *Inorg. Chem.* **2015**, *54*, 6606; E. E. Langdon-Jones, N. O. Symonds, S. E. Yates, A. J. Hayes, D. Lloyd, R. Willi-ams, S. J. Coles, P. N. Horton, S. J. A. Pope, *Inorg. Chem.* **2014**, *53*, 3788.

[13] For example, A. J. Amoroso, M. P. Coogan, J. E. Dunne, V. Fernandez-Moreira, J. B. Hess, A. J. Hayes, D. Lloyd, C. Millet, S. J. A. Pope, C. Williams, *Chem. Commun.* **2007**, 3066; A. W.-T. Choi, M.-W. Louie, S. P.-Y. Li, H.-W. Liu, B. T.-N. Chan, T. C.-Y. Lam, A. C.-C. Lin, S.-H. Cheng, K. K.-W. Lo, *Inorg. Chem.* **2012**, *51*, 13289; A. Palmioli, A. Aliprandi, D. Septiadi, M. Mauro, A. Bernardi, L. De Cola, M. Panigati, *Org. Biomol. Chem.* **2017**, *15*, 1686; V. Fernandez-Moreira, M. L. Ortego, C. F. Williams, M. P. Coogan, M. D. Villacampa, M. C. Gimeno, *Organometallics* **2012**, *31*, 5950; E. E. Langdon-Jones, A. B. Jones, C. F. Williams, A. J. Hayes, D. Lloyd, H. J. Mottram, S. J. A. Pope, *Eur. J. Inorg. Chem.* **2017**, 759; R. G. Balasingham, F. L. Thorp-Greenwood, C. F. Williams, M. P. Coogan, S. J. A. Pope, *Inorg. Chem.* **2012**, *51*, 1419; A. J. Amoroso, R. J. Arthur, M. P. Coogan, J. B. Court, V. Fernan-dez-Moreira, A. J. Hayes, D. Lloyd, C. Millet, S. J. A. Pope, *New J. Chem.* **2008**, *32*, 1097.

[14] K. de Oliveira, P. Costa, J. Santin, L. Mazzambani, C. Burger, C. Mora, R. Nunes, M. de Souza, *Bioorg. Med. Chem.* **2011**, *19*, 4295.

[15] L. A. Mullice, S. J. A. Pope, *Dalton Trans.* **2010**, *39*, 5908.

[16] F. L. Thorp-Greenwood, M. P. Coogan, A. J. Hallett, R. H. Laye, S. J. A. Pope, *J. Organomet. Chem.* **2009**, *694*, 1400.

[17] Z. Y. Wu, J. N. Cui, X. H. Xian, T. Y. Liu, *Chin. Chem. Lett.* **2013**, *24*, 359.

[18] M. Wrighton, D. L. Morse, *J. Am. Chem. Soc.* **1974**, *96*, 998.

[19] D. R. Striplin, G. A. Crosby, *Coord. Chem. Rev.* **2001**, *211*, 163.

[20] http://www.molinspiration.com.

[21] V. Fernandez-Moreira, F. L. Thorp-Greenwood, A. J. Amoroso, J. Cable, J. B. Court, V. Gray, A. J. Hayes, R. L. Jenkins, B. M. Kariuki, D. Lloyd, C. O. Millet, C. F. Williams, M. P. Coogan, *Org. Biomol. Chem.* **2010**, *8*, 3888.

[22] S. J. Coles, P. A. Gale, *Chem. Sci.* **2012**, *3*, 683.

[23] *CrystalClear-SM Expert 3.1 b27*, **2013**, Rigaku.

[24] O. V. Dolomanov, L. J. Bourhis, R. J. Gildea, J. A. K. Howard, H. Puschmann, *J. Appl. Crystallogr.* **2009**, *42*, 339.

[25] L. Palatinus, G. Chapuis, *J. Appl. Crystallogr.* **2007**, *40*, 786.

[26] G. M. Sheldrick, *Acta Crystallogr., Sect. C* **2015**, *71*, 3.

[27] P. van der Sluis, A. L. Spek, *Acta Crystallogr., Sect. A* **1990**, *46*, 194.

[28] see ref.[14].

[29] S. P. Schmidt, W. C. Trogler, F. Basolo, M. A. Urbancic, J. R. Shipley, "Penta-carbonylrhenium Halides" in *Inorganic Syntheses: Reagents for Transition Metal Complex and Organometallic Syntheses* (Ed.: R. J. Angelici), John Wiley & Sons, Hoboken, **2007**, p. 160.